PHOTOMASK

BACUS—The international technical group of SPIE dedicated to the advancement of photomask technology.

3rd Place Winner for Best Oral Presentation - SPIE Photomask Technology 2014

Performance of GFIS mask repair system for various mask materials

Fumio Aramaki, Tomokazu Kozakai, Osamu Matsuda, Anto Yasaka, Hitachi High-Tech Science Corporation, 36-1 Takenoshita, Oyama-cho, Sunto-gun, Shizuoka 410-1393, Japan

Shingo Yoshikawa, Koichi Kanno, Hiroyuki Miyashita, Naoya Hayashi, Dai Nippon Printing Co., Ltd., 2-2-1 Fukuoka, Fujimino-shi, Saitama 356-8507, Japan

ABSTRACT

We have developed a new focused ion beam (FIB) technology using a gas field ion source (GFIS) for mask repair. Meanwhile, since current high-end photomasks do not have high durability in exposure nor cleaning, some new photomask materials are proposed. In 2012, we reported that our GFIS system had repaired a representative new material "A6L2". It is currently expected to extend the application range of GFIS technology for various new materials and various defect shapes. In this study, we repaired a single bridge, a triple bridge and a missing hole on a phase shift mask (PSM) of "A6L2", and also repaired single bridges on a binary mask of molybdenum silicide (MoSi) material "W4G" and a PSM of high transmittance material "SDC1". The etching selectivity between those new materials and quartz were over 4:1. There were no significant differences of pattern shapes on scanning electron microscopy (SEM) images between repair and non-repair regions. All the critical dimensions (CD) at repair regions were less than +/-3% of those at normal ones on an aerial image metrology system (AIMS). Those results demonstrated that GFIS technology is a reliable solution of repairing new material photomasks that are candidates for 1X nm generation.

1. Introduction

1.1 Background

A scanning microscope of helium ion (He^+) emitted by GFIS is well known as a novel tool for high resolution imaging and processing.[1,2] We have also investigated the applicability of GFIS technology to FIB systems for mask repair.

Meanwhile, in proportion to shrinkage of device design rule, exposure wavelength has been shortened and new mask materials have been introduced into semiconductor photolithography. For the past ten years, EUVL has been referred to be the most promising candidate for 1X nm generation. It was reported that EB repaired EUVL masks.[3,4] We also reported that EUVL masks can be repaired with hydrogen ions ($H2^+$) emitted by GFIS.[5] However, since EUVL light sources are still in the developing stage now, we will have no option but to use photomasks for 1X nm generation for the present. On the other hand, current high-end photomasks are very expensive, but those lives are not so long due to reduction of those films during exposure and cleaning.

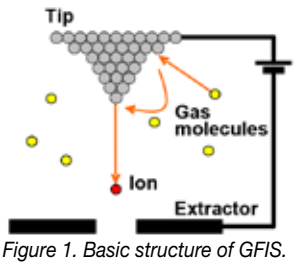

Figure 1. Basic structure of GFIS.

$$D = 2R = 2\sqrt{(MRs)^2 + \left(\frac{1}{4}C_{si}\alpha_i^{\,3}\right)^2 + \left(\frac{1}{2}C_{ci}\alpha_i\frac{\Delta E}{E}\right)^2}$$

D : Beam diameter
R : Beam radius
M : Magnification
Rs : Source size
α_i : Beam cone angle
C_{si} : Spherical aberration coefficient
C_{ci} : Chromatic aberration coefficient
E : Acceleration voltage
ΔE : Energy spread

BACUS NEWS

April 2015
Volume 31, Issue 4

SPIE.

9235-14

EDITORIAL

Mask CD Metrology: Are we keeping up?

By **Tom Faure,** IBM Corporation

As we continue to push the limits of optical lithography to the 10 nm logic node and transition to the use of EUV lithography at the 7 nm logic node the challenges of fully characterizing the mask critical dimension (CD) performance are increasing. Not only do we have to worry about measuring traditional items such mask CD mean to target and across mask CD uniformity (CDU) to tighter specifications, but we also need to measure and assess 2D structures on the mask such as line ends, corner rounding, and complex OPC hot spots. In addition it is becoming increasingly important to measure the sidewall angle of the mask absorbers for both optical and EUV masks. In taking a look at these mask metrology requirements it is not clear that the current mask equipment and infrastructure is keeping up.

Let's start by considering mask CD uniformity. The ITRS road map indicates that the across mask CD uniformity requirement for optical and EUV masks is approaching 1 nm (3 sigma) in 2015 and 2016. 10 nm node critical level optical masks typically have a 1.2 nm (3 sigma) specification and critical level EUV masks for 7 nm lithography require a 1 nm (3 sigma) spec. As these CD uniformity specifications tighten the percentage of the spec that is taken up by the short term and long term repeatability performance of the mask SEMs used to measure CDU increases. For example today's mask CD SEMs have typical repeatability of 0.3 nm on lines and spaces, and therefore metrology noise takes up 30% of a 1 nm CDU spec. For comparison, state of the art SEMs used in wafer fabs typically have 0.2 nm repeatability on 1D line structures. Measuring across mask CDU on the dot and hole structures on contact and via level masks is an even bigger challenge due to the use of much smaller ROI (region of interest) sizes which results in significantly worse metrology repeatability and makes it much less likely to meet a 1 nm CDU spec. Use of multiple ROIs in a single field of view (FOV) on contact/via structures has helped improve measurement performance (increased averaging), but this is not a viable option for measuring isolated contact/via structures across the mask.

Improvement in our ability to measure small features on masks is needed. Advanced optical masks have SRAFs (sub-resolution assist features) as small as 45 nm, and EUV masks have main feature sizes as small as 70 nm with a CD mean to target requirement of + or – 1 nm . However, most mask SEMs are still being used at 50 k and 75 k magnifications and have very limited capability above 100 k. In contrast to this, the state of the art wafer SEMs routinely perform measurements at 300 k magnification and are used at magnifications as high as 450 k. Below are SEM images taken at 75 k of a 90 nm x 90 nm opaque dot and 50 nn line feature on an advanced optical mask and a 107 nm contact hole on an EUV mask. At this 75k magnification the field of view is 1920 nm. Clearly an increase in the magnification and correspondingly an increase in resolution would improve the measurement of these images. If we take into account that there are typically 1024 x 1024 pixels in the 1920 nm field of view on the current mask SEM systems this gives us a resolution of 1.875 nm per pixel. For comparison most wafer SEMs perform measurements at a resolution of 0.5- 0.8 nm per pixel with some measurements being done at resolutions as high as 0.3 nm per pixel. At a 100 k magnification the field of view on a mask SEM is 1440 nm which makes high resolution measurement of 70 nm and 45 nm features and features with complex OPC (small jogs, notches and nubs) a challenge. The limited capability of mask SEM tools above 100 k magnification is due to the negative impact of increased charging and shadowing effects caused by the underlying thick quartz substrate on optical masks. Additional improvements in mask SEM tool hardware are needed to reduce these charging and shadowing effects to enable routine use of higher magnification on optical masks. EUV masks exhibit much less charging in the CD SEM and should be easier to image at higher magnifications if the SEM systems are designed to support it. In addition to improving CD SEM capability for measuring small features on EUV masks, high resolution SEM images of EUV masks are also needed to analyze and measure line edge roughness (LER) of the absorber sidewall since high LER on the mask will transfer to the wafer.

90 nm dot and 50 nm line at 75kx on optical mask and 107 nm contact hole on EUV mask. Field of view is 1920 nm.

(continued on page 7)

BACUS

N • E • W • S

BACUS News is published monthly by SPIE for BACUS, the international technical group of SPIE dedicated to the advancement of photomask technology.

Managing Editor/Graphics Linda DeLano
Advertising Lara Miles
BACUS Technical Group Manager Pat Wight

SPIE.

P.O. Box 10, Bellingham, WA 98227-0010 USA
Tel: +1 360 676 3290
Fax: +1 360 647 1445
www.SPIE.org
help@spie.org

Table 1. Specifications of our developed GFIS system.

Ion species	For photomask	Nitrogen (N_2^+)
	For EUV mask	Hydrogen (H_2^+)
Acceleration voltage (ACC)		15 - 30 keV
Probe current (Ip)		0.1 - 1.0 pA
Field of view (FOV)		1 - 300 μm
Sample interface		SMIF
Defect recognition		Automatic

Figure 2. Appearance of our GFIS system.

In order to break through the above situation, mask blank manufacturers are proposing various new photomask materials. "A6L2" is a MoSi phase shift mask and a representative product among the above new materials. We reported that an A6L2 masks can be repaired with nitrogen ions ($N2^+$) emitted by GFIS.[6] It was also reported that EB repaired A6L2 masks.[7] It is currently expected to repair defects of other shapes and other new materials that neither GFIS nor EB has evaluated.

1.2 Objective of this study

The objective of this study is to verify that GFIS technology is applicable to repairing defects of various shapes on the above new material masks that are candidates for 1X nm generation. In the concrete, we evaluated etching material selectivity, etching shapes, AIMS CD and through-focus behaviors.

2. Methods

2.1 Principle of GFIS

Fig.1 shows a basic structure of GFIS. Ambient gas molecules around a tip are ionized and accelerated by an electric field generated between the tip and an extractor. The beam diameter of focused ion beam is generally expressed by the following equation. The source size (*Rs*) of GFIS is much smaller than that of conventional liquid metal ion sources (LMIS), because ions of GFIS are generated in a field of a few atoms. The energy spread (ΔE) of GFIS is much smaller than that of LMIS, because gas molecules are ionized in a narrow range of particular electric field intensity. Thus the beam diameter (*D*) of GFIS is much smaller than that of LMIS.

2.2 Experimental system

We developed a new mask repair system by using GFIS. Fig.2 shows the appearance of that system. That system can emit nitrogen and hydrogen ions by replacing gas molecules around a tip. Nitrogen ions ($N2^+$) are used to repair photomasks. Hydrogen ions ($H2^+$) are used to repair EUV masks. The design of the other functions except the GFIS is greatly modified from our conventional FIB systems. The main specifications are listed in Table 1.

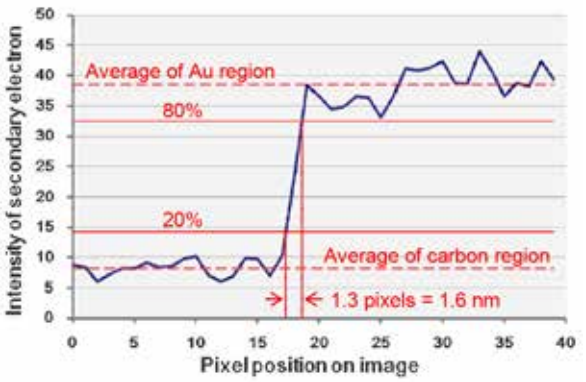

Figure 3. GFIS secondary electron intensity of an Au particle on a carbon substrate ($N2^+$ beam, ACC=25kV, Ip =0.1pA).

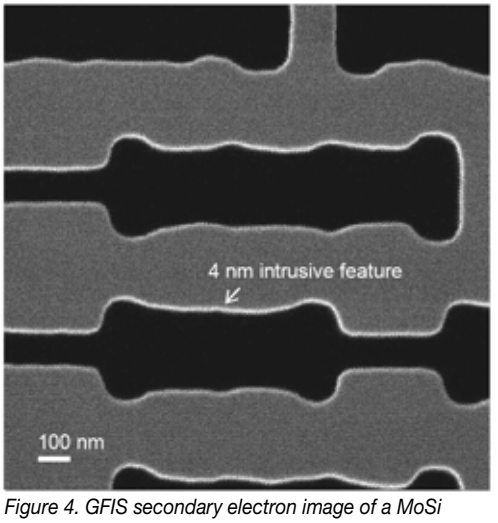

Figure 4. GFIS secondary electron image of a MoSi mask ($N2^+$ beam, ACC=25kV, Ip=0.1pA, FOV=1.5um).

2.3 Basic capability of experimental system

Before the evaluation of this study, we confirmed the basic capability of the above GFIS system.

In order to confirm image resolution, we had observed gold (Au) particles on a carbon substrate. Fig.3 shows the secondary electron intensity profile with $N2^+$ beam, 25 kV acceleration voltage (ACC) and 0.1 pA probe current (Ip). From the width of a slope between an Au region and a carbon one, its image resolution is calculated to be 1.6 nm.

In order to confirm image quality, we observed holes with optical proximity correction (OPC) on an A6L2 mask. Fig.4 shows the secondary electron image with $N2^+$ beam, 25 kV ACC, 0.1 pA Ip and 1.5 um field of view (FOV). A 4 nm intrusive feature is recognized at the edge of a hole. There is high contrast between MoSi film and quartz.

In order to confirm the minimum etching width, we cut a groove in an A6L2 film with $N2^+$ beam, 25 kV ACC, 0.1 pA Ip and 1-line scanning as shown in Fig.5. Fig.6 shows its SEM images. The width of the groove is 8.9 nm. The sidewall of the groove is almost perpendicular.

In order to confirm repair position accuracy, we etched 30 nm extruded defects on a conventional MoSi mask ten times with $N2^+$

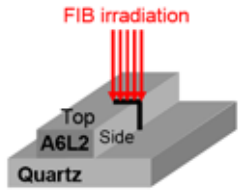

Figure 5. Sample making method of a 1-line etching sample.

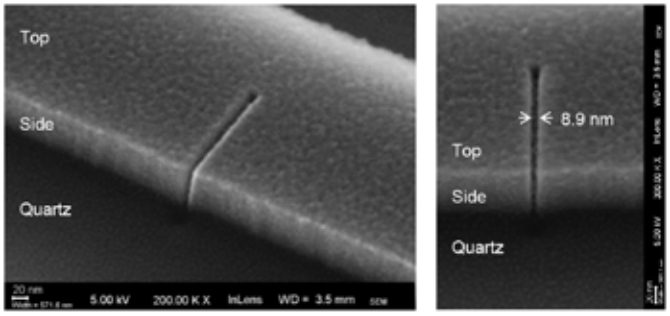

Figure 6. SEM images of a MoSi film after 1-line etching with our GFIS system (N2⁺ beam, ACC=25kV, Ip=0.1pA).

Table 2. Sample masks in this study.

Sample	Type	Model	Manufacturer
1	High durable MoSi phase shift	A6L2	HOYA
2	MoSi binary	W4G	Shin-Etsu
3	High transmittance phase shift	SDC1	Shin-Etsu

Table 3. Evaluation tools in this study.

Evaluation	Type	Model	Manufacturer
Etching shape	SEM	E3620	Advantest
Etching depth	AFM	Dimension X3D	Veeco
Optical characteristics	AIMS	AIMS32-193i	Carl Zeiss

beam, 25 kV ACC, 0.1 pA Ip and 2.0 um FOV as shown in Fig.7. Those repair position errors were measured on GFIS images as shown in Fig.8. The standard deviation of those errors is calculated to be 0.62 nm. If repair position accuracy is defined as three times the deviation, it is calculated to be 1.85 nm.

2.4 Sample masks and evaluation tools

We repaired defects on the new material masks as listed in Table.2. One representative product is selected from each kind of candidates for 1X nm generation masks. After repairs, etching shape, depth and optical characteristics of those masks were evaluated with the tools as listed in Table.3.

3. Results

3.1 Etching material selectivity

New film materials (A6L2, W4G, SDC1) and quartz were etched with various doses of 25 kV accelerated nitrogen ions ($N2^+$) as shown Fig.9. The depths of those etching regions are measured with an atomic force microscope (AFM). Fig.10 shows the correlation between ion doses and etching depths. The etching rates of A6L2, W4G, SDC1 and quartz are calculated to be 0.092, 0.043, 0.048 and 0.010 nm3/ion. Thus etching selectivity of A6L2, W4G and SDC1 to quartz are calculated to be 9.0 : 1, 4.7 : 1 and 4.2 : 1.

3.2 Repair shape of L/S on A6L2

A single bridge defect at lines and spaces (L/S) on an A6L2 mask

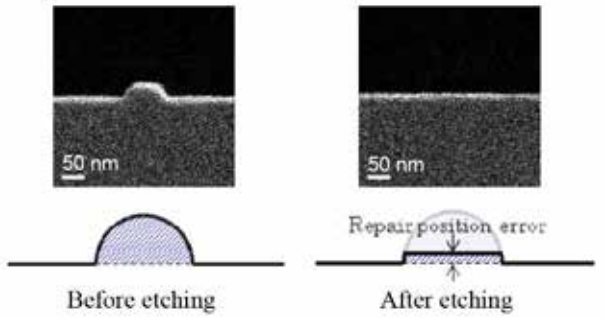

Figure 7. Sample making and measuring method of repair position samples (GFIS images).

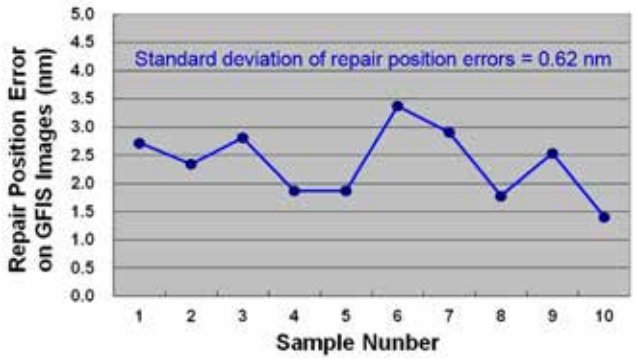

Figure 8. Repair position error on GFIS images.

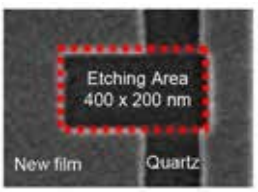

Figure 9. Sample making method (N2⁺ beam, ACC=25kV).

was repaired with $N2^+$ beam. The half pitch (HP) of the L/S is 180 nm on the mask. The size of that defect is 180 x 720 nm on the mask. That defect was observed with SEM before and after repairing as shown in Fig.11. There are no significant differences between repair and non-repair regions on the SEM images. The major characteristics of the repair shapes are as follows.

- ✎ Neither riverbed nor residue on the bottom
- ✎ No protruding residue on the repair edges
- ✎ Sharp shoulders of the repair edges

3.3 AIMS results of L/S repair on A6L2

In order to verify that CDs at the upper and lower ends of the above defect are the same as CD at the center, CDs at those three points were measured with AIMS. All the three CD errors are less than +/-3% through +/-1.25 um (wafer dimension) defocus as shown in Fig.12. In order to verify that CD after cleaning is the same as CD before cleaning, CD after cleaning was measured with AIMS. There are only about 1% differences between CDs before and after cleaning. Fig.13 shows the AIMS analysis results at the center. There are no significant differences between the repair region and normal ones on the intensity profile. The correlation curves between thresholds and CDs at the repair region closely resemble ones that are typically seen at normal regions.

3.4 Application to contact holes and large defects

In order to verify that GFIS is applicable to other shapes except single bridge defects, a missing hole and a triple bridge defect on an A6L2 mask were repaired with $N2^+$ beam. The size of holes is 350 x 350 nm on the mask. The HP of the L/S is 180 nm on the mask. The defects were observed with SEM as shown in Fig.14 and 16. There are no significant differences between repair and non-repair regions on the SEM images. CDs after repairing were measured with AIMS as shown in Fig.15 and 17. All the CD errors are less than +/-3% through +/-1.25 um (wafer dimension) defocus.

3.5 Repair capability to W4G and SDC1

In order to verify that GFIS has capabilities to repair other new materials except A6L2, single bridge defects on W4G and SDC1 masks were repaired with $N2^+$ beam. The HP of the L/S is 180 nm on the masks. The size of the defects is 180 x 720 nm on the masks. The defects were observed with SEM as shown in Fig.18 and 20. There are no significant differences between repair and non-repair regions on the SEM images. CDs after repairing were measured with AIMS as shown in Fig.19 and 21. All the CD errors are less than +/-3% through +/-1.25 um (wafer dimension) defocus.

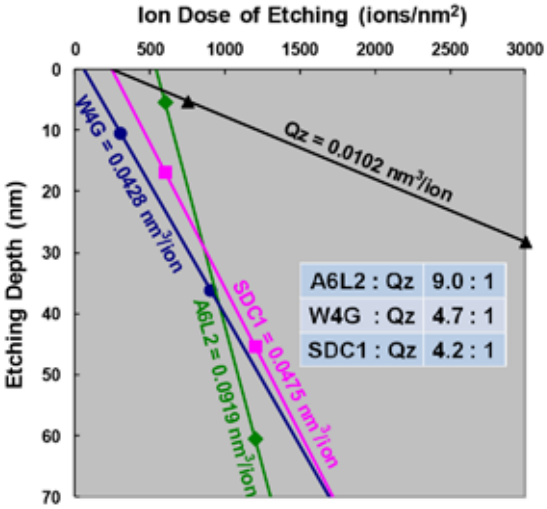

Figure 10. Etching rates of A6L2, W4G, ADC1 and quartz ($N2^+$ beam, ACC=25kV).

4. Conclusions

We developed the new FIB mask repair system equipped with GFIS and evaluated its performance to repair A6L2, W4G and SDC1 that are candidates for 1X nm generation masks. The main results obtained in this study are listed below. Those results demonstrate that GFIS technology is a reliable solution of repairing those new masks.

- Etching selectivity of A6L2, W4G and SDC1 to quartz is over 4:1.
- There are no significant differences of pattern shapes on SEM images between repair and non-repair regions.
- AIMS CD errors* after repairing a single bridge, a triple bridge and a missing hole on an A6L2 mask are less than +/-3%.
- AIMS CD errors* after repairing single bridge defects on W4G and SDC1 masks are less than +/-3%.
- There are no significant differences between AIMS results of the repair region on an A6L2 mask before cleaning and those after it.

*AIMS CD errors were measured through +/-1.25 um (wafer dimension) defocus.

5. Acknowledgments

The authors thank HOYA CORPORATION, Shin-Etsu Chemical Co., Ltd., Beam technology system design section of Hitachi High-Tech Science Corporation and the mask process development team at Kamifukuoka plant of Dai Nippon Printing Co., Ltd.

6. References

[1] B. W. Ward et al., "Helium ion microscope: A new tool for nanoscale microscopy and metrology", *J. Vac. Sci. Technol.* B 24, 2871 (2006).

[2] D. Maas et al., "Nanofabrication with a helium ion microscope", **Proc. SPIE 7638,** 763814 (2010).

[3] S. Kanamitsu et al., "Prospect of EUV mask repair technology using e-beam tool", **Proc. SPIE 7823,** 782322 (2010).

[4] R. Jonckheere et al., "Repair of natural EUV reticle defects", **Proc. SPIE 8186,** 81661G (2011).

[5] F. Aramaki et al., "Development of new FIB technology for EUVL mask repair", **Proc. SPIE 7969,** 79691C (2011).

[6] F. Aramaki et al., "Photomask repair technology by using gas field ion source", **Proc. SPIE 8441,** 84410D (2012).

[7] S. Kanamitsu et al., "Application of EB repair for high durable MoSi PSM", **Proc. SPIE 9256,** 92560U (2014).

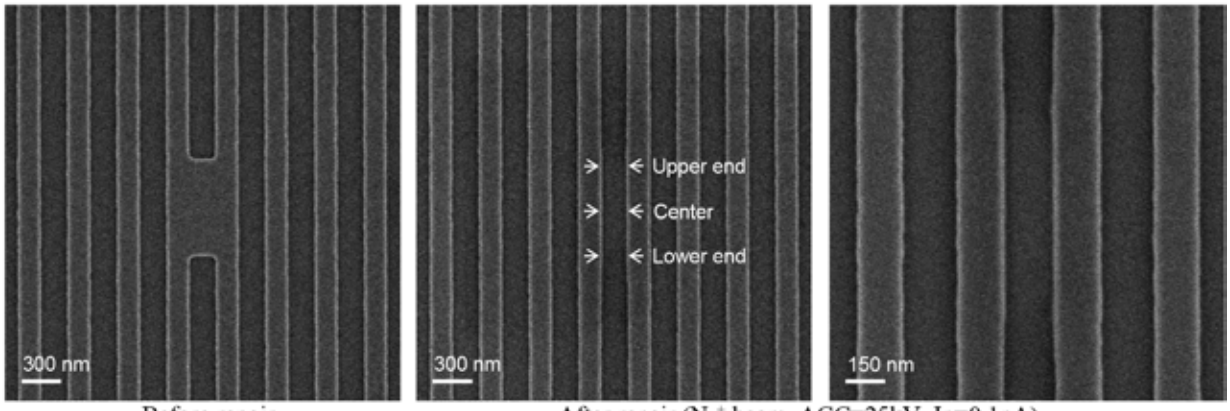

Figure 11. SEM images of a bridge defect at 180 nm HP (mask dimension) L/S on an A6L2 mask.

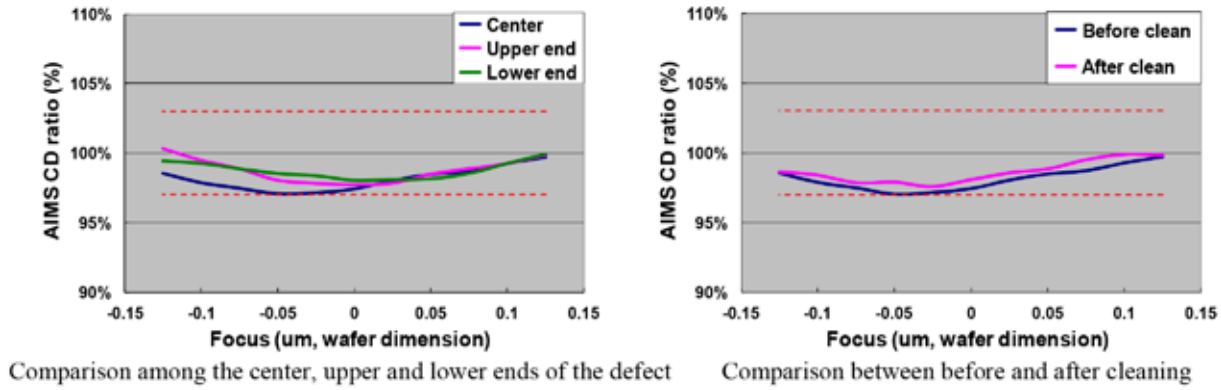

Figure 12. AIMS CD errors after repairing a bridge defect at 180 nm HP (mask dimension) L/S on an A6L2 mask.

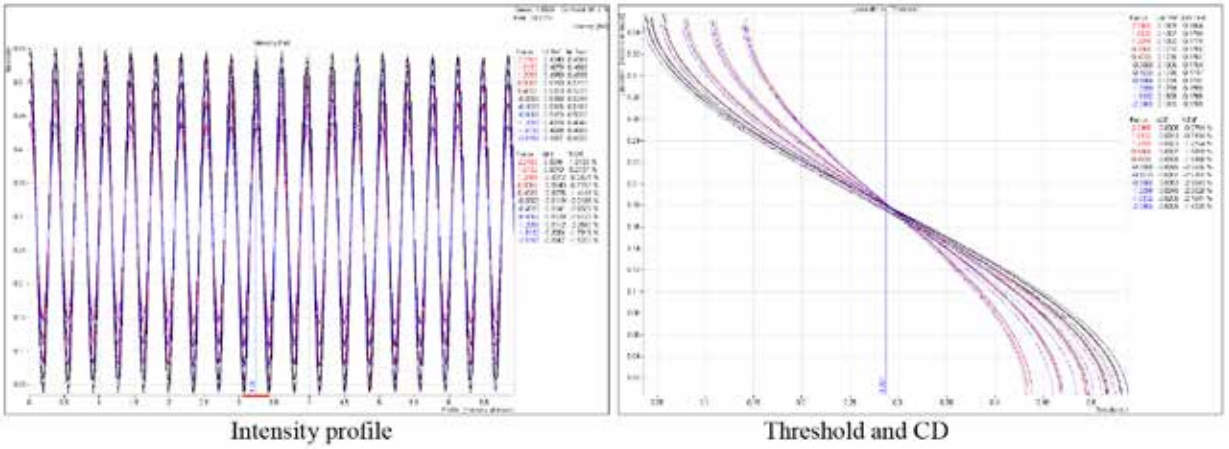

Figure 13. AIMS analysis results after repairing a bridge defect at 180 nm HP (mask dimension) L/S on an A6L2 mask.

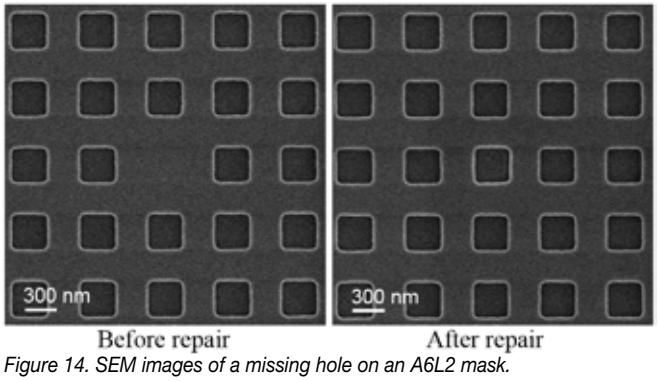

Figure 14. SEM images of a missing hole on an A6L2 mask.

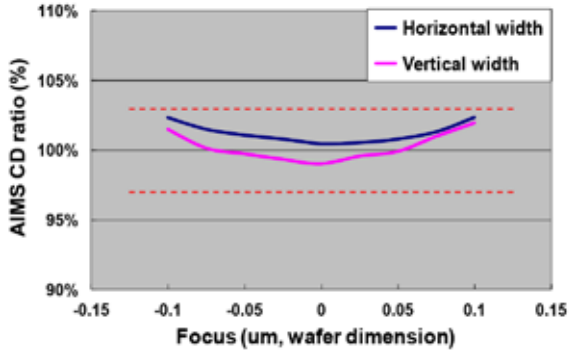

Figure 15. AIMS CD after repairing a missing hole on an A6L2 mask.

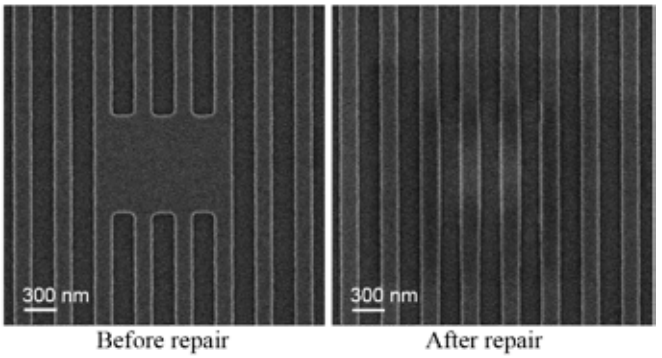

Figure 16. SEM images of a triple bridge defect on an A6L2 mask.

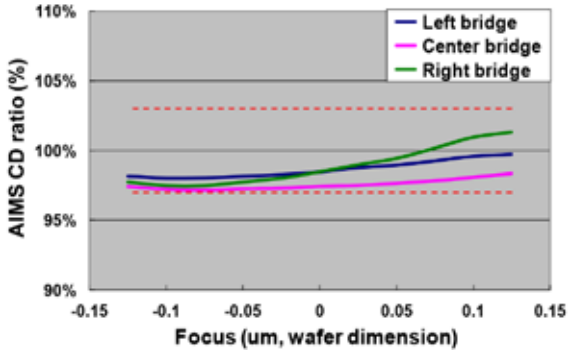

Figure 17. AIMS CD after repairing a triple bridge defect on an A6L2.

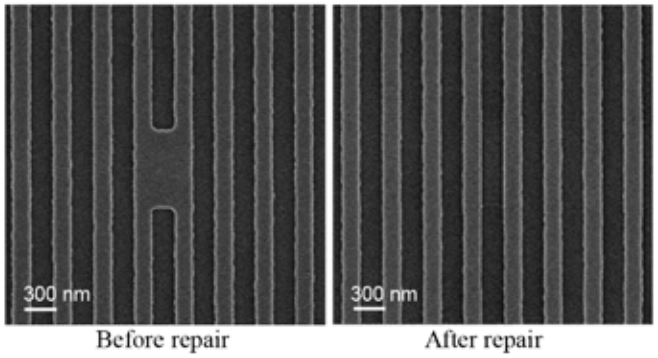

Figure 18. SEM images of a bridge defect on a W4G mask.

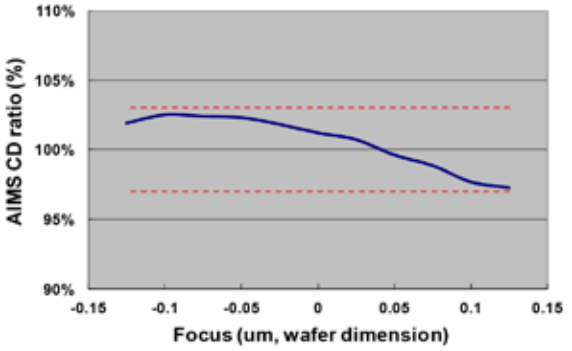

Figure 19. AIMS CD after repairing a bridge defect on a W4G mask.

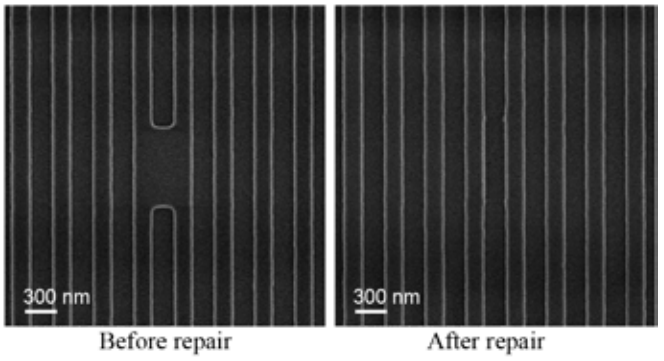

Figure 20. SEM image of a bridge defect on a SDC1 mask.

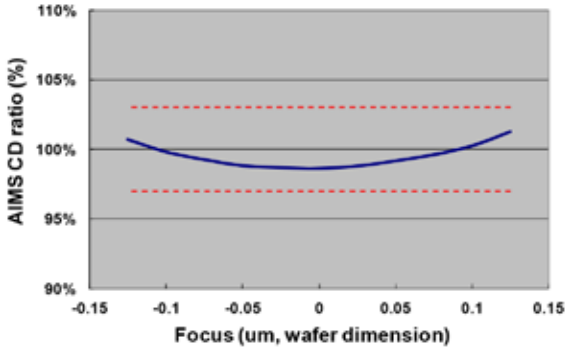

Figure 21. AIMS CD after repairing a bridge defect on a SDC1 mask.

EDITORIAL *(continued from page 2)*

Improved accuracy is becoming increasingly important for advanced mask metrology. At older technology nodes mask CD measurement accuracy for mean to target was largely ignored and was buried in the OPC model. I can remember back at 130 nm node we switched from measuring masks using an optical transmitted light technique to SEM and saw a 60 nm shift in the measured CD. The wafer lithography engineers at the time told us not to compensate for this CD shift and insisted that we continue to send masks as if they were measured on the optical tool. In addition they affectionately coined a new term called the "maskron" for the unit of measure of our reported mask CD measurement values. At the 10 nm and 7 nm logic nodes the accuracy of mask CD mean to target measurements is crucial for enabling the most accurate lithography models possible. The lithography models all assume accurate mask CD's for both main features and SRAF features, and therefore lack of mask CD accuracy becomes a source of error in the models. Unfortunately there does not appear to be a universal linewidth standard for masks that is being used by the industry. Some mask shops use their own internal linewidth standard for tool calibration while other mask shops use a pitch standard instead of a linewidth standard. This lack of consistency has led to large offsets in mask metrology between mask shops (up to 30-40 nm) and has made CD matching amongst multiple mask shops quite challenging. In addition, offsets between AFM and mask CD SEM of 10-15 nm are not uncommon. These types of offsets are too large to be ignored due to the small feature sizes that are required on today's advanced masks.

Measurement of complex OPC structures and 2d line end, tip to tip and corner rounding structures is another challenging area for mask CD metrology. The new mask CD metrology systems that generate and measure an aerial image from the mask have been helpful for measuring the 2d and complex OPC structures and have been a welcome addition to mask CD metrology. These systems have demonstrated the potential to show good correlation to actual wafer printing results at the 28 nm and 20 nm nodes and have the benefit of including the effects of the mask absorber sidewall, mask topography effects, mask LER, phase, and MEEF in the measured aerial image . However, improvement in the repeatability and accuracy of these systems is needed for 10 nm optical masks. Unfortunately this type of aerial image metrology option currently does not exist for EUV masks but may in the future with the new EUV AIMSTM systems. The aggressive OPC with its small jogs, notches and nubs on today's optical masks makes it extremely difficult to measure real device structures and 2D tip to tip performance on the mask using CD SEM due to the very small ROI sizes and limited capability of the pattern recognition systems to insure that measurements are done at the correct location in the field of view. The very recent adaptation of the design based metrology (DBM) approach used by the wafer SEMs by one of the mask SEM manufacturers is improving the capability of the mask SEMs to measure these more complicated structures at low magnification.

Since EUV masks rely on changes in reflectivity to create images on wafer, they require detailed characterization and measurement of the sidewall angle of the patterned absorber that is covering the reflective multilayer substrate. In addition, today's OPC models for advanced optical masks require a thorough understanding and measurement of the sidewall angle of the attenuator film as a critical input parameter into the OPC model. Mask shops are starting to use AFM (atomic force microscopy) tools for characterizing the sidewalls of the attenuator films. However, the tip life of AFM probes is very short when used on EUV masks due to the hardness of the tantalum absorber film. In many cases the AFM tips wear out after 30 touches. In addition it is very challenging to get reasonable sidewall angle results with AFM in small trenches (< 100 nm) on the mask. The 3D imaging capabilities available on the newest mask SEM equipment is still a work in progress and is not yet ready for routine use to accurately and repeatably measure sidewall angles. Scatterometry is another potential method for monitoring sidewall performance on masks in a production environment, but it requires a large and time consuming resource investment to build models and libraries for each different mask absorber film.

In order to meet the CD metrology requirements for advanced optical and EUV masks, mask makers, equipment suppliers, and software vendors will need to work together to continue to develop improved mask CD metrology capability and potentially leverage the capabilities that already exist in the wafer fabs. Otherwise we are at risk of not keeping up with the needs of our advanced lithography partners and customers. Furthermore, the industry needs to come to agreement on a common linewidth standard for optical and EUV masks to improve metrology accuracy.

BACUS N • E • W • S

Sponsorship Opportunities

Sign up now for the best sponsorship opportunities

Photomask 2015 —
Contact: Lara Miles, Tel: +1 360 676 3290; laram@spie.org

Advanced Lithography 2016 —
Contact: Lara Miles, Tel: +1 360 676 3290; laram@spie.org

Advertise in the BACUS News!

The BACUS Newsletter is the premier publication serving the photomask industry. For information on how to advertise, contact:

Lara Miles
Tel: +1 360 676 3290
laram@spie.org

BACUS Corporate Members

Acuphase Inc.
American Coating Technologies LLC
AMETEK Precitech, Inc.
Berliner Glas KGaA Herbert Kubatz GmbH & Co.
FUJIFILM Electronic Materials U.S.A., Inc.
Gudeng Precision Industrial Co., Ltd.
Halocarbon Products
HamaTech APE GmbH & Co. KG
Hitachi High Technologies America, Inc.
JEOL USA Inc.
Mentor Graphics Corp.
Molecular Imprints, Inc.
Panavision Federal Systems, LLC
Profilocolore Srl
Raytheon ELCAN Optical Technologies
XYALIS

Industry Briefs

2015 SPIE Advanced Lithography EUVL Conference – Summary and Analysis

Vivek Bakshi, EUV Litho, Inc., Semiconductor International, March 2015

The SPIE AL EUVL Conference (February 22-26, 2015, San Jose, CA) enjoyed a positive atmosphere toward EUVL, based on a lot of new data.

Scanner status

The latest NXE 3300B EUVL scanner with an 80 watt EUV source, ran continuously for over 24 hours and processed more than 1000 Wafers, in a dramatic improvement from last year, at 10W source power barrier. Machine to machine overlay and mix and match overlay (with immersion tools) continue to improve too. TSMC also showed line and space with 15 nm half pitch and 14nm trenches. ASML pointed out that 3300B scanners now meet the patterning requirement for the 7nm logic node and 15nm DRAM node. Hynix can now use EUVL scanners with "sufficient productivity with better or comparable yield" compared to immersion scanners.

EUV Pellicle

The industry now plans to use pellicles to protect the EUV mask from defects added during manufacturing. For ASML full size pellicles with 85% single pass transmission (30% total loss), the transmission is supposed to increase to 90% this year (20% total loss). These pellicles can now be shipped worldwide without breakage. The pellicles do not interfere with imaging as they have a negligible effect on CD uniformity (CDU) and line edge roughness (LER).

High NA Scanner and optics

Optics quality (wave front error and flare), scanner optics throughput, and illumination schemes continue to improve due to Carl Zeiss efforts. Numerical aperture (NA) for scanners needs to increase to further increase resolution – ASML has 0.5 NA on their roadmap beyond 10nm HP.

EUV Source

Cymer has an in-house 100 W source which operates with 3.5 % conversion efficiency (CE), 15 kW drive laser and 17% overhead cost (meaning only 87% of the light output is used to ensure required dose control). With a master oscillatory power amplifier (MOPA) and pre-pulse based system, they hope to get 5.5 % CE with a 27 kW CO2 drive laser. This proposed switch should give them a factor of 2.6 over current source power or ~ target of 250W.

Gigaphoton announced 142W at 50% duty cycle (71 W average power) source operated at 4.2 % CE and 70 KHZ in a burst mode for a short time. They have ~15 days availability of debris mitigation scheme and their approach is to obtain 250W in burst mode and work on improving the source availability.

EUV Resists

Due to strict outgassing requirements to protect the scanner optics, it takes a long time to get a new EUV resist evaluated in the EUVL scanner. For non-CAR chemistries, up to 100 wafers can be processed in the EUVL scanner before needing outgas testing certificate to continue. There is now lot more focus on negative-tone CAR resists for EUV for meeting the resist requirements.

The current commercial HfO_2 based resist show a shelf life of three to four weeks only. Metal oxide based EUV resists, which due to high absorption property, can dramatically reduce EUV dose requirements and hence relax source power requirements, are not quite ready for production. High sensitivity HfO_2 (2.2 mJ) and ZrO_2 (1.8 mJ) resists had LER of ~ 6nm. The nano-aspect of these metal resists does not make it more toxic and they have passed outgassing tests at IMEC.

EUV Masks

Although mask defectivity continues to drop, more work is needed to reach acceptable mask blank defect levels. The magnetron technology, although still behind IBD in terms of defectivity, provides better reflectivity and better manufacturability. Also, mask pattern shift is the method that is increasingly being employed to reduce defects in patterned masks.

Alternate multilayer materials for masks support higher NA scanners (Ru/Si multilayer with carbon interlayer instead of Mo/Si), which will allow less shadowing and hence smaller through-focus pattern placement errors.

Mask Defect Inspection

Carl Zeiss plans to deliver an AIMS tool in Q4 of 2015 to support mask defect repair, and chip makers are discovering alternate ways to find defects on patterned mask, while an actinic patterned mask defect inspection tool is not available. Even with a pellicle, EUV patterned masks may still have defects generated during production from handling, or from contamination trapped between masks and pellicles. Although existence and frequency of these defects has still not been proven, chip makers will prefer to have a through pellicle actinic inspection.

So When EUVL Will Reach HVM?

Per the ASML roadmap, the throughput of NXE3350 at 125 W is ~ 75 Wafers per hour (WPH), and with two 3300Bs being upgraded to 3350 levels and two new 3350 scanners operational at TSMC this year, TSMC can hope for throughput ~ 300 WPH later this year from their four NXE3350 EUVL scanners. As source power climbs to 250W in these scanners, throughput per scanner will climb to 125 WPH, or 500 WPH for four scanners indicating the capability for moving beyond product development, perhaps in 2016 or at the latest 2017.

Join the premier professional organization for mask makers and mask users!

About the BACUS Group

Founded in 1980 by a group of chrome blank users wanting a single voice to interact with suppliers, BACUS has grown to become the largest and most widely known forum for the exchange of technical information of interest to photomask and reticle makers. BACUS joined SPIE in January of 1991 to expand the exchange of information with mask makers around the world.

The group sponsors an informative monthly meeting and newsletter, BACUS News. The BACUS annual Photomask Technology Symposium covers photomask technology, photomask processes, lithography, materials and resists, phase shift masks, inspection and repair, metrology, and quality and manufacturing management.

Individual Membership Benefits include:

- Subscription to BACUS News (monthly)
- Eligibility to hold office on BACUS Steering Committee

www.spie.org/bacushome

Corporate Membership Benefits include:

- 3-10 Voting Members in the SPIE General Membership, depending on tier level
- Subscription to BACUS News (monthly)
- One online SPIE Journal Subscription
- Listed as a Corporate Member in the BACUS Monthly Newsletter

www.spie.org/bacushome

Calendar

2015

SPIE Photomask Technology
29 September-1 October 2015
Monterey Marriott and
Monterey Conference Center
Monterey, California, USA
www.spie.org/pm

Co-located with
SPIE Scanning Microscopies
www.spie.org/sg

2016

SPIE Advanced Lithography
San Jose Convention Center
and San Jose Marriott
San Jose, California, USA
www.spie.org/al

SPIE Advanced Lithography call will be available late April 2015.

SPIE is the international society for optics and photonics, a not-for-profit organization founded in 1955 to advance light-based technologies. The Society serves nearly 225,000 constituents from approximately 150 countries, offering conferences, continuing education, books, journals, and a digital library in support of interdisciplinary information exchange, professional growth, and patent precedent. SPIE provided over $3.4 million in support of education and outreach programs in 2014.

SPIE.
International Headquarters
P.O. Box 10, Bellingham, WA 98227-0010 USA
Tel: +1 360 676 3290
Fax: +1 360 647 1445
help@spie.org • www.SPIE.org

Shipping Address
1000 20th St., Bellingham, WA 98225-6705 USA

Managed by SPIE Europe
2 Alexandra Gate, Ffordd Pengam, Cardiff,
CF24 2SA, UK
Tel: +44 29 2089 4747
Fax: +44 29 2089 4750
spieeurope@spieeurope.org • www.spieeurope.org

You are invited to submit events of interest for this calendar. Please send to lindad@spie.org; alternatively, email or fax to SPIE.